European Journal of Radiology 86 (2017) 227–233

Contents lists available at ScienceDirect

European Journal of Radiology

journal homepage: www.elsevier.com/locate/ejrad

Optimal timing of image acquisition for arterial first pass CT myocardial perfusion imaging

G.J. Pelgrim[a], E.R. Nieuwenhuis[a,b], T.M. Duguay[c], R.J. van der Geest[d], A. Varga-Szemes[c], C.H. Slump[a,b], S.R. Fuller[c], M. Oudkerk[a], U.J. Schoepf[c], R. Vliegenthart[a,c,*]

[a] University of Groningen, University Medical Center Groningen, Center for Medical Imaging North East Netherlands (CMI-nen), Hanzeplein 1, 9713 GZ Groningen, The Netherlands
[b] University of Twente, P.O. Box 217, 7500 AE, Enschede, The Netherlands
[c] Medical University of South Carolina, Dept. of Radiology, 25 Courtenay Drive, SC 29425, Charleston, United States
[d] Leiden University Medical Center, Dept. of Radiology, Postbus 9600, 2300 RC, Leiden, The Netherlands

ARTICLE INFO

Article history:
Received 1 April 2016
Received in revised form
28 September 2016
Accepted 22 November 2016

Keywords:
Tomography
X-Ray computed
Myocardial perfusion imaging
Iodine
Ischemia

ABSTRACT

Purpose: To determine the optimal timing of arterial first pass computed tomography (CT) myocardial perfusion imaging (CTMPI) based on dynamic CTMPI acquisitions.
Methods and materials: Twenty-five patients (59 ± 8.4 years, 14 male)underwent adenosine-stress dynamic CTMPI on second-generation dual-source CT in shuttle mode (30 s at 100 kV and 300 mAs). Stress perfusion magnetic resonance imaging (MRI) was used as reference standard for differentiation of non-ischemic and ischemic segments. The left ventricle (LV) wall was manually segmented according to the AHA 16-segment model. Hounsfield units (HU) in myocardial segments and ascending (AA) and descending aorta (AD) were monitored over time. Time difference between peak AA and peak AD and peak myocardial enhancement was calculated, as well as the, time delay from fixed HU thresholds of 150 and 250 HU in the AA and AD to a minimal difference of 15 HU between normal and ischemic segments. Furthermore, the duration of the 15 HU difference between ischemic and non-ischemic segments was calculated.
Results: Myocardial ischemia was observed by MRI in 10 patients (56.3 ± 9.0 years; 8 male). The delay between the maximum HU in the AA and AD and maximal HU in the non-ischemic segments was 2.8 s [2.2–4.3] and 0.0 s [0.0–2.8], respectively. Differentiation between ischemic and non-ischemic myocardial segments in CT was best during a time window of 8.6 ± 3.8 s. Time delays for AA triggering were 4.5 s [2.2–5.6] and 2.2 s [0–2.8] for the 150 HU and 250 HU thresholds, respectively. While for AD triggering, time delays were 2.4 s [0.0–4.8] and 0.0 s [−2.2–2.6] for the 150 HU and 250 HU thresholds, respectively.
Conclusion: In CTMPI, the differentiation between normal and ischemic myocardium is best accomplished during a time interval of 8.6 ± 3.8 s. This time window can be utilized by a test bolus or bolus tracking in the AA or AD using the time delays identified here.

Abbreviations: CCTA, coronary computed tomography angiography; CAD, coronary artery disease; CT, computed tomography; MPI, myocardial perfusion imaging; SPECT, single photon emission computed tomography; MRI, magnetic resonance imaging; ICA, invasive coronary angiography; HU, Hounsfield unit; AA, ascending aorta; AD, descending aorta; ECG, electrocardiography; LV, left ventricle; MPR, multiplanar reformat reconstructions; AHA, American Heart Association; TAC, time-attenuation curves; ROIs, regions of interest.

* Corresponding author at: University of Groningen, University Medical Center Groningen, Center for Medical Imaging–North East Netherlands, Hanzeplein 1, P.O. Box EB44, 9713 GZ Groningen, The Netherlands.
E-mail addresses: g.j.pelgrim@umcg.nl (G.J. Pelgrim), e.r.nieuwenhuis@student.utwente.nl (E.R. Nieuwenhuis), duguay@musc.edu (T.M. Duguay), R.J.van_der_Geest@lumc.nl (R.J. van der Geest), vargaasz@musc.edu (A. Varga-Szemes), c.h.slump@utwente.nl (C.H. Slump), fullerst@musc.edu (S.R. Fuller), m.oudkerk@umcg.nl (M. Oudkerk), schoepf@musc.edu (U.J. Schoepf), r.vliegenthart@umcg.nl (R. Vliegenthart).

http://dx.doi.org/10.1016/j.ejrad.2016.11.024
0720-048X/

1. Introduction

Coronary computed tomography angiography (CCTA) is a reliable modality for the diagnosis of anatomical coronary artery disease (CAD) with a high negative predictive value [1,2]. However, assessing the hemodynamic significance of intermediate stenosis using CCTA is often challenging, as the effect of luminal narrowing on myocardial perfusion varies. Non-invasive techniques for myocardial perfusion imaging (MPI) are used to analyse the hemodynamic significance of a stenosis. These include single photon emission computed tomography (SPECT), magnetic resonance imaging (MRI) and invasive techniques (e.g. invasive coronary angiography (ICA) with fractional flow reserve measurement) [3]. With recent advances in CT technology, CT-based MPI emerges as an additional approach for the evaluation of the myocardial blood supply [4–10].

In CTMPI, an iodinated contrast agent is administered through an intravenous catheter and the subsequent distribution of the iodine contrast through the myocardium is evaluated. The CT assessment of the myocardial blood supply can be accomplished via two different scanning approaches: (1) a dynamic scan mode in which data are acquired at multiple time points, and (2) a static single-shot acquisition during first arterial pass. In the dynamic mode, the contrast enhancement of the myocardium is analyzed at multiple time points during the first-pass of the contrast, enabling calculation of myocardial blood flow over time and assessment of the true myocardial perfusion. In this scan mode, the table is shuttling between two scanning positions. The coverage of the dynamic scan mode is 7.3 cm, 2 times the detector size of 3.8 cm minus a 10% overlap between both scan positions. This method has an approximate time resolution of 2–3 s using dual-source CT scanners, acquiring images every second or third heartbeat. However, the increased number of acquisitions required with dynamic scanning results in a relatively high radiation dose, compared to static, single-shot techniques [8]. Although, radiation dose has come down in recent years, implementation into clinical practice is still in research phase.

As an alternative, the static, single-shot technique provides the myocardial iodine contrast distribution at a single point in time during first arterial pass. As a result, the single-shot technique cannot provide quantitative values for myocardial perfusion parameters. However, the static method can determine Hounsfield Unit (HU) differences between myocardial segments resulting from hemodynamically significant stenosis. Accurate timing of scan acquisition to yield optimal contrast differentiation between normal and ischemic myocardium is ensured through either a test bolus technique or bolus tracking approaches [11,12]. However, only one study analyzed the optimal timing of static perfusion CT scans in patients [13]. The need to establish optimal time delays remains in order to develop standardized static stress CT perfusion protocols. As such, the aim in this study was to define the optimal time delays for static single-shot CTMPI protocols during first arterial pass using different trigger points (AA and AD) and different trigger approaches (test bolus and bolus tracking).

2. Methods and materials

In this retrospective single-center study, we analyzed 26 patients with suspicion of CAD who had undergone dynamic CTMPI and adenosine stress perfusion MRI between November 2009 and July 2011 as part of a research protocol. The study protocol was approved by the local Institutional Review Board and informed consent was obtained from each patient. The study was conducted in HIPAA compliance. Stress MRI was used as reference standard. Two separate studies were performed: (1) a base study in which CT time delays were determined in the non-ischemic segments of all patients, and (2) a sub-study in 10 patients with perfusion defects indicated by stress MRI. In the latter, the optimal time delay for the differentiation between ischemic and non-ischemic segments on dynamic CT perfusion analysis was determined at three different slice locations: basal, mid-ventricular and apical.

2.1. MRI myocardial perfusion acquisition protocol

Patients were scanned on a 1.5-T MRI system (Magnetom Avanto; Siemens, Erlangen, Germany). Imaging parameters used for acquisition of perfusion images were: repetition time 2.8 ms; echo time 1.21 ms; flip angle 50°; field-of-view 380 × 80.2 mm; temporal resolution 150 ms; and slice thickness 10 mm. The protocol covered 3 short-axis slices (basal, mid-ventricular and apical) of the left ventricle (LV) in each heartbeat for 50 consecutive heartbeats. Gadopentate dimeglumine (Magnevist: 0.5 mol/L; Bayer-Schering, Berlin, Germany) was used as contrast agent at a dosage of 0.2 mL/kg per scan. Contrast was administered at 4 mL/s, followed by 15 mL saline chaser. Stress MPI was performed under infusion of adenosine (Adenoscan, Astellas, Tokyo, Japan; 140 μg/kg/min). Rest perfusion scanning was performed 10 min after stress scanning. Two experienced readers in consensus evaluated results of MRI MPI to determine ischemic and non-ischemic segments by visual analysis of first-pass perfusion defects using a picture archiving and communication system (Agfa Impax, Agfa Healthcare, Greenville, SC, USA). MR results were used as a reference for CTMPI assessment.

2.2. CT myocardial perfusion acquisition protocol

Dynamic CT perfusion was performed on a second-generation dual-source CT scanner (SOMATOM Definition Flash, Siemens, Forchheim, Germany). Stress imaging was performed 3 min after start of adenosine infusion with a dose of 140 μg/kg/min. Iopromide (Ultravist 370, Bayer AG, Berlin, Germany) was injected as a contrast bolus of 40–50 mL at an injection rate of 4–6 mL/s, resembling an iodine delivery rate ranging from 1.5 to 2.2 g/s, followed by a saline chaser. Data were acquired in shuttle mode, where the table is moving back and forth between two scanning positions. Scans were acquired using electrocardiographic (ECG) triggering at end-systole (250 ms after R-peak), with a tube voltage of 100 kV for both tubes, gantry rotation time of 280 ms, and a tube current of 300 mAs per rotation. Detector range of the scanner was 38 mm, and, with an overlap of 10%, resulted in a total z-volume coverage of 73 mm. Scans were started 4 s prior to contrast arrival in the heart to allow baseline non-contrast acquisition and total scan time was 30 s. Scan delay for the dynamic stress acquisition was determined using a test bolus.

2.3. CT myocardial perfusion analysis

MASS software (Research version 5.1, Leiden University Medical Center, Leiden, Netherlands) was used to evaluate CTMPI studies (Fig. 1). Cross sectional multiplanar reformat reconstructions (MPR) of 10 mm thickness were created at the basal, mid-ventricular and apical planes of the LV myocardium. In each individual heart, spacing between the three different MPR slices (basal, mid-ventricular and apical) was kept constant, varying between 8 and 26 mm for different patients, taking differences in LV size into account. The American Heart Association (AHA) 17-segment model was used to draw the myocardial segments[14]. The apical segments were excluded from the analysis, resulting in 16 analyzed myocardial segments per patient. Epicardial and endocardial contours were drawn manually by a researcher with 4 years of experience. Each slice was automatically divided into either six or four segments; six segments for basal and midventricular slices and four segments for

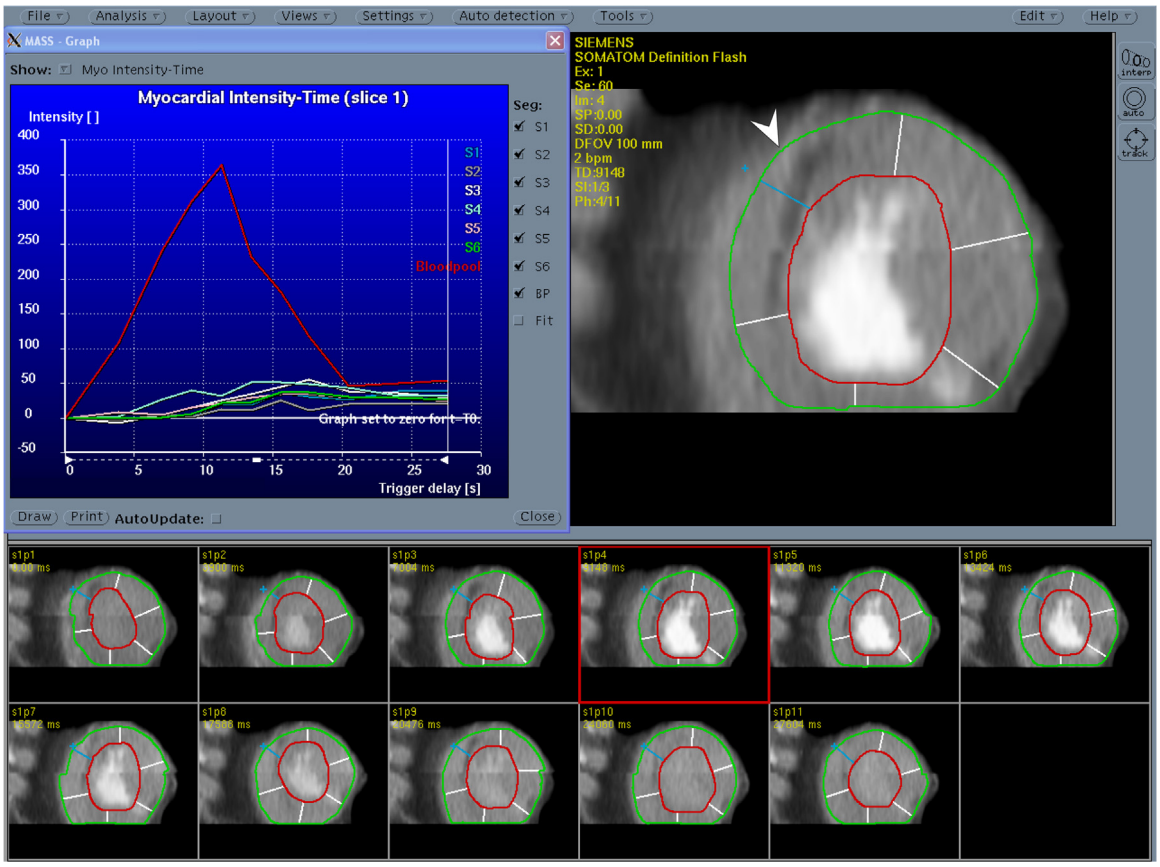

Fig. 1. Evaluation of the myocardial segments performed in the MASS research software. On the left side, the enhancement in HU is shown for the separate myocardial segments and the blood pool. The white arrow shows a perfusion defect in septal wall. The bottom images show the different time stamps for the same slice location.

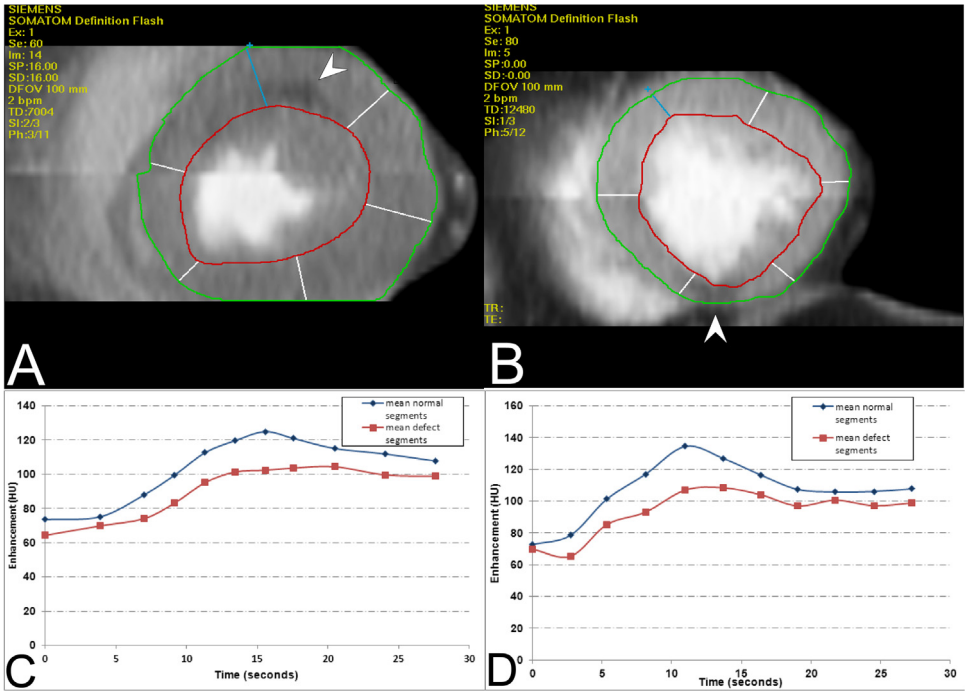

Fig. 2. The arrows in image A and B point to two perfusion defects in two separate patients. Graphs C and D show the difference between the mean HU enhancement in two graphs for the ischemic and non-ischemic segments of patient A and patient B, respectively.

apical slices. Mean contrast density in Hounsfield units (HU) was determined in the 16 myocardial segments at all time points in all patients (Fig. 2). Additionally, HU attenuation in possible trigger locations were derived by drawing regions of interest (ROIs) in the

standard transversal plane in the AA and AD using the Aquarius iNtuition Viewer (Version 4.1.11, TeraRecon Inc, Foster City, USA). The AA ROI was drawn at the proximal part of the AA, because of the limited scan range.

In order to determine contrast delays between trigger locations and myocardial segments, several timestamps were calculated. A timestamp was defined as the time point corresponding to the moment of acquisition. For myocardial segments, timestamps were determined for max HU enhancement ($maxTP_{MYO}$) for each slice location in each patient. Furthermore, timestamps were calculated for a minimal difference of 15 HU between ischemic and non-ischemic segments ($TP_{diff > 15}$) for each slice location, only in patients with ischemia. Myocardial segments with ischemia were determined based on gold standard MR perfusion results. In cases where the HU difference was <15HU, the point in time where HU difference was highest was used as $TP_{diff>15}$. Slices without a perfusion defect were excluded from this part of the analysis. Timestamps in both trigger locations (AA and AD) were determined for both max HU ($maxTP_{AA}$, $maxTP_{AD}$) and pre-defined HU thresholds of 150 HU and 250 HU (AA_{150} and AA_{250}; AD_{150} and AD_{250}), resulting in six timestamps ($maxTP_{AA}$, TP_{AA150}, TP_{AA250}; $maxTP_{AD}$, TP_{AD150}, TP_{AD250}).

The time difference between peak HU enhancement in the trigger locations ($maxTP_{AA}$, $maxTP_{AD}$) and maximum enhancement in myocardial segments ($maxTP_{MYO}$) was calculated for all separate slice locations (e.g. basal, mid-ventricular and apical) in all patients. In patients with ischemia, the time difference between trigger location timestamps TP_{AA150}, TP_{AA250}, TP_{AD150}, TP_{AD250} and $TP_{diff > 15}$ was calculated for all slices with a perfusion defect. In addition, the duration of the >15 HU difference between ischaemic and non-ischaemic myocardial segments at each slice location was determined in all patients.

2.4. Statistical analysis

Statistical analysis was performed using SPSS 23 (IBM Corp, Armonk, NY). All determined time delays were analyzed for normality by skewness and kurtosis testing. Data were reported as median [interquartile ranges] or mean ± SD.

3. Results

3.1. Patient inclusion

Twenty-five patients (14 male, 59 ± 8.4 years) were included in the analysis and one patient was excluded due to missing data. Ten patients (56.3 ± 9 years; 8 males) had myocardial ischemia detected by the reference adenosine stress perfusion MRI. These patients were included in the time-delay analysis for optimal differentiation between ischemic and non-ischemic segments.

3.2. Optimal timing overall

Time delay between maximal HU enhancement in the AA, $maxTP_{AA}$, and maximal HU enhancement in the non-ischemic segments, $maxTP_{MYO}$, had a median value of 2.8 s [2.2–4.3] (Fig. 3 and Table 1). For $maxTP_{AD}$ to $maxTP_{MYO}$, median time delay for maximal enhancement was 0.0 s [0.0–2.8]. For TP_{AA150}, median time interval between the AA threshold and peak enhancement in myocardial segments was 7.7 s [6.1–9.4], and for TP_{AA250}, delay was 5.6 s [4.8–7.2]. For TP_{AD150}, median time interval from the 150 HU threshold in the AD to peak enhancement in the myocardium was 6.2 s [5.2–8.5] and for TP_{AD250}, median time interval was 4.7 s [2.8–6.4].

3.3. Optimal timing for differentiating normal and ischemic segments

Based on the data from patients with ischemic myocardial segments, median time delay from TP_{AA150} to $TP_{diff > 15}$ was 4.5 s [2.2–5.6], whereas a threshold of 250 HU in the AA resulted in a shorter time delay, 2.2 s [0–2.8]. For the AD, median time delay was 2.4 s [0.0–4.8] for the 150 HU threshold and 0.0 s [−2.2–2.6] for the 250 HU threshold (Fig. 4 and Table 1). Optimal differentiation between ischemic and non-ischemic myocardium was present for 8.6 ± 3.8 s (Fig. 5). The optimal time frame for maximal differentiation was approximately 4 s after the AA threshold of 150 HU and 2 s after the 150 HU threshold in the AD. This window of optimal HU contrast was present for approximately 8 s, in the case of a contrast bolus of 40–50 mL at an injection rate of 4–6 mL/s. The median highest HU difference per patient was 21.4 with a percentile range from 18.1 to 36.2 and a total range from 14 to 61 HU.

4. Discussion

In the current study, we analyzed the time delays for optimal timing of single-shot CTMPI, based on dynamic CT perfusion data. In this study we showed that there is an approximate time window of 8.5 s in which the HU difference between ischemic and non-ischemic segments is optimal. Furthermore, the separate delays for AA and AD triggering were analyzed. Using the proposed delays, optimal differentiation for single-shot CT perfusion can be achieved.

Previous studies have determined the time delay for optimal contrast between ischemic and non-ischemic segments from predefined trigger points based on dynamic CTMPI studies in dogs and patients [13,15]. Both studies reported an optimal time interval for discrimination between ischemic and non-ischemic segments of 6 s–12 s. The current study confirms and expands the results of the 2 prior studies. Our results are in accordance with these findings, with an optimal time window of 8.6 ± 3.8 s observed in our investigation. However, the time point of maximum difference between ischemic and non-ischemic segments does not necessarily correspond to the start of the recognisable HU differences between ischemic and non-ischemic segments. In addition, the AD may be preferable for triggering compared to the AA as it is less affected by motion. Therefore, ROIs were placed in the AA and AD to study the time delays for separate trigger locations, which was not performed in the study by Bischoff et al. Furthermore, the time delays found in our study were shorter compared to the ones reported by Bischoff et al. In the subgroup analysis (n = 10), the TP_{AA150}–$TP_{diff > 15}$ time interval was 2.5 s shorter compared to the delay suggested in that latter investigation.

In non-ischemic myocardial segments, the time delay between the threshold of 150 HU in the AA and AD and peak enhancement in the myocardium was 7.7 s and 6.2 s, respectively. When compared to the time delays found for the scans with HU difference >15, a single-shot scan can be started before peak enhancement in the myocardium, because ischemic defects can be quantified during the build-up of contrast in the myocardium. An explanation for the difference between both studies could lie in the injection protocol and differences in cardiac output between patients. In clinical practice, the injection protocol is often dependent on multiple parameters, (e.g. patient size, tube current, iodine concentration in contrast media, etc.).

Two reference locations were analyzed in order to provide insight on suitable trigger locations. The time delay difference between AA and AD for the trigger thresholds is 1.5–3 s in most cases, resembling one shuttle interval. The time difference between maximum HU enhancement in the specified trigger point and peak

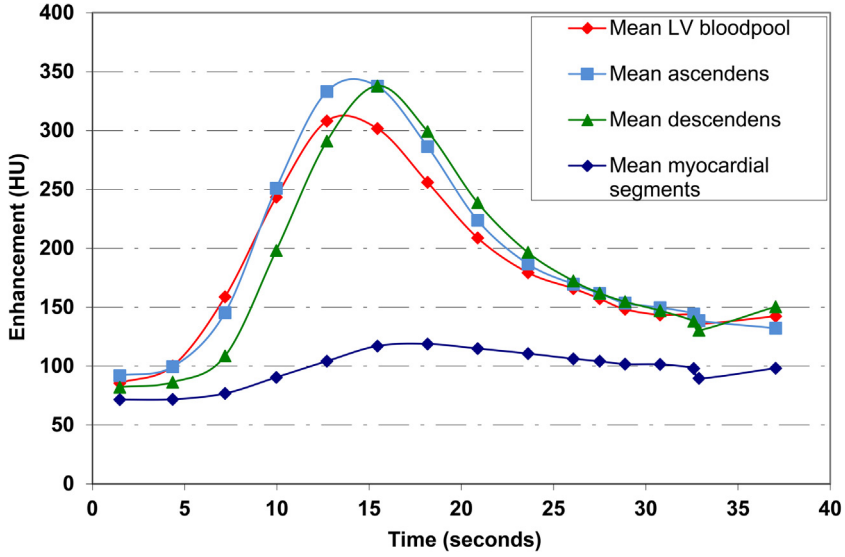

Fig. 3. Enhancement in HU on the Y-axis for left ventricular blood pool, ascending aorta, descending aorta and the average of the non-ischemic myocardial segments. Top enhancement in the descending aorta is, on average, at the same instant as the top HU enhancement in the myocardial segments.

Table 1
Median time interval between the time stamps in the myocardium ($maxTP_{myo}$ and $TP_{diff > 15}$) and the time stamps in both reference locations (TP_{AA150}, TP_{AA250}, $maxTP_{AA}$; TP_{AD150}, TP_{AD250}, $maxTP_{AD}$) is displayed, as well as the interquartile range.

Time difference	TP_{AA150}	TP_{AA250}	$MaxTP_{AA}$	TP_{AD150}	TP_{AD250}	$maxTP_{AD}$
$maxTP_{MYO}$	7.7 s[6.1–9.4]	5.6 s[4.8–7.2]	2.8 s[2.2–4.3]	6.2 s[5.2–8.5]	4.7 s [2.8–6.4]	0.0 s[0.0–2.8]
$TP_{diff > 15HU}$	4.5 s[2.2–5.6]	2.2 s [0–2.8]	n.a.	2.4 s[0.0–4.8]	0.0 s[−2.2–2.6]	n.a.

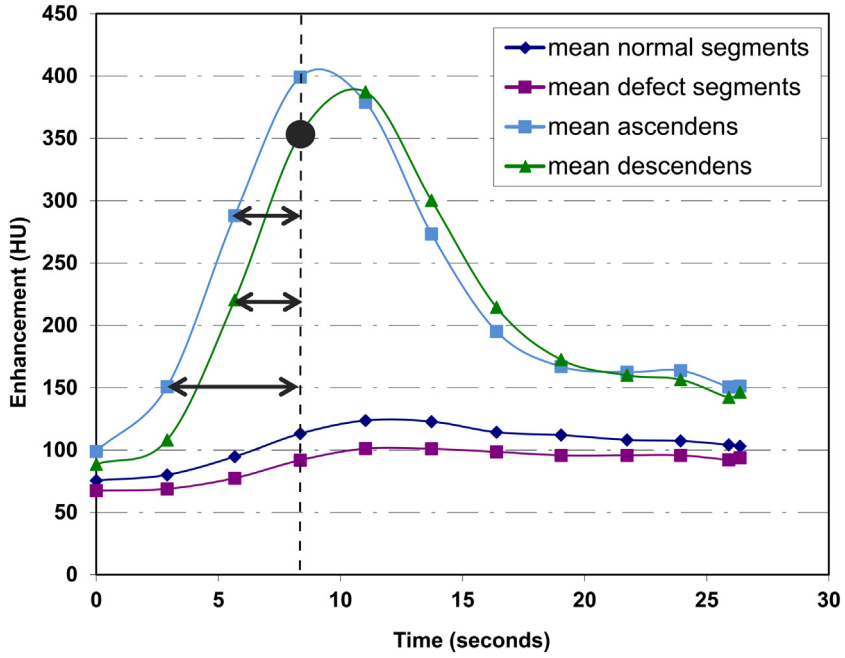

Fig. 4. An example of the HU enhancement graphs shows the difference between mean non-ischemic and ischemic segments. From the dotted line onward, HU differences between ischemic and non-ischemic segments are larger than 15 HU. For the ascending aorta, 150 HU threshold has an average delay of 4 s and the 250 HU threshold has a 2 s delay. For the descending aorta, 150 HU threshold has an average 2 s delay and the 250 HU threshold has a 0 s delay. The black arrows point out the separate delays for the ascending and descending aorta at both the 150 and 250 HU threshold.

HU enhancement in myocardial segments was 3 s (AA) 0 s (AD). This suggests that one could use the AD peak enhancement to plan fast myocardial perfusion scanning using the test bolus technique. A test bolus can be used to determine the time delay between the injection time and arterial enhancement in AA or AD. However, bolus length alteration should be taken into account when determining CT perfusion scan delay. The HU peak enhancement in the myocardial segments is often comparable to peak AD HU enhancement, however this rule does not apply perfectly for every patient. In our study, the minimal and maximal time delay was −7.1 s and

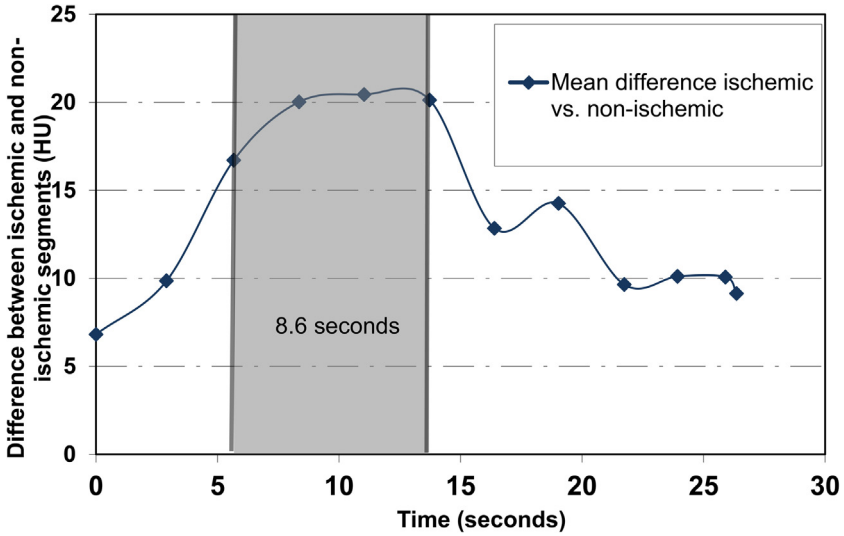

Fig. 5. The mean difference between the ischemic and non-ischemic segments is shown on the Y-axis. Best HU differentiation between ischemic and non-ischemic segments is present for the duration of 8.6 s.

8.7 s, respectively. In those cases, upslope contrast enhancements are comparable, but peak value time can have large time differences between individuals. Furthermore, peak enhancement in the myocardium does not automatically imply the greatest difference between ischemic and non-ischemic segments.

In patients with a perfusion defect, the AA median time delays for 150 HU and 250 HU thresholds were 4.5 s [2.2–5.6] and 2.2 s [0–2.8], respectively. A threshold in one of the reference locations (AA or AD) can be used for bolus tracking of the single-shot perfusion scan [12]. In order for this technique to work, the locations should be stable, quantifiable and contrast enhancement should not be too late compared to the contrast enhancement in the myocardial segments. In case of late contrast enhancement in the reference location, the CT scanner will not have enough time to prepare and perform the myocardial perfusion scan [12]. So, the AA reference ROI trigger can be used with both a threshold of 150 HU and 250 HU, which results in an optimal contrast window of 4–12 s and 2–10 s, respectively. Triggering in the AD should only be performed with a low HU threshold of 150 HU, within a time window from 2 to 10 s after the 150 HU threshold has been reached.

The maximal difference in the myocardium is present for approximately 8 s, in which the total heart should be scanned. Such scanning parameters are feasible with newer generation scanners [8]. Along with previous studies, these results could guide future CT perfusion studies in order to acquire optimal contrast between normal and ischemic myocardial segments. There are multiple options for snapshot CTMPI imaging during first arterial pass, e.g., dual energy, high-pitch spiral, and sequential approaches [8]. Dual energy could have an edge on other static techniques due to its ability to quantify the iodine concentration at one point in the cardiac cycle [16,17]. A dual energy scan can be acquired within the 8 s window of greatest difference between ischemic and non-ischemic myocardium. High-pitch spiral modes are fast imaging modes with low radiation dose, but are prone to imaging artefacts in case of irregular or high heart rates. In sequential mode, images are acquired using a step and shoot technique. This technique is slower because it takes several heart beats to acquire the image, but is less prone to motion artefacts. Thus, depending on the patient, different trigger and imaging modes could perform best to acquire myocardial perfusion analysis at the most suitable interval of tissue attenuation.

There are several limitations to this study. Because of the shuttle mode, images were acquired at different time points. This is contributing to the large standard deviation, because one time point will already result in an effective time difference between 1 and 3 s [8]. Furthermore, in our study the injection protocol differed between patients based on patient characteristics. This could be an explanation for the difference between the results of our study and Bischoff's. However, this reflects clinical practice. Another limitation of the second generation dual source CT system is the 7.3 cm scan range. In some of the patients, the LV cannot be fully imaged. Therefore, some of the segments could not be analyzed and were excluded from either the mean HU of the ischemic or non-ischemic segment analysis. Furthermore, the sample size of patients with a perfusion defect in this study was limited. Of the 25 patients, only 10 had a proven perfusion defect on MRI which could be matched with the dynamic CT data.

Dynamic CT perfusion analysis is still a long way from being implemented into daily clinical practice in European countries. However, in Asian countries this technique is already routinely used in clinical practice. Still, single-shot CTMPI techniques, prone to less radiation exposure, are potentially able to assess myocardial contrast enhancement [8,17]. The addition of functional assessment to the anatomical evaluation of CAD by CTA has the potential to provide diagnosis using a single imaging technique.

5. Conclusion

In conclusion, the best differentiation between ischemic and non-ischemic myocardium can be made in static CTMPI during a time interval of 8.6 ± 3.8 s. The optimal time delay for static CTMPI using an AA trigger location was 4 s (150 HU) and 2 s (250 HU). Using the trigger location in the AD, 2 s (150 HU) time delay was optimal.

Conflict of interest

U.J. Schoepf is a consultant for and/or receives research support from Astellas, Bayer, Bracco, GE, Guerbet, Medrad, and Siemens. The other authors have no conflict of interest to disclose.

Acknowledgement

R. Vliegenthart is supported by a grant from the Netherlands Organisation for Scientific Research.

References

[1] J. Abdulla, S.Z. Abildstrom, O. Gotzsche, E. Christensen, L. Kober, C. Torp-Pedersen, 64-Multislice detector computed tomography coronary angiography as potential alternative to conventional Coronary angiography: a systematic review and meta-analysis, Eur. Heart J. 28 (24) (2007) 3042–3050.

[2] E.A. Hulten, S. Carbonaro, S.P. Petrillo, J.D. Mitchell, T.C. Villines, Prognostic value of cardiac computed tomography angiography: a systematic review and meta-analysis, J. Am. Coll. Cardiol. 57 (10) (2011) 1237–1247.

[3] C. Jaarsma, T. Leiner, S.C. Bekkers, et al., Diagnostic performance of noninvasive myocardial perfusion imaging using single-photon emission computed tomography, cardiac magnetic resonance, and positron emission tomography imaging for the detection of obstructive coronary artery disease: a meta-analysis, J. Am. Coll. Cardiol. 59 (19) (2012) 1719–1728.

[4] A.H. Mahnken, E. Klotz, H. Pietsch, et al., Quantitative whole heart stress perfusion CT imaging as noninvasive assessment of hemodynamics in coronary artery stenosis: preliminary animal experience, Invest. Radiol. 45 (6) (2010) 298–305.

[5] F. Schwarz, R. Hinkel, E. Baloch, et al., Myocardial CT perfusion imaging in a large animal model: comparison of dynamic versus single-phase acquisitions, JACC Cardiovasc. Imaging 6 (12) (2013) 1229–1238.

[6] F. Bamberg, R. Hinkel, R.P. Marcus, et al., Feasibility of dynamic CT-based adenosine stress myocardial perfusion imaging to detect and differentiate ischemic and infarcted myocardium in an large experimental porcine animal model, Int. J. Cardiovasc. Imaging 30 (4) (2014) 803–812.

[7] G.J. Pelgrim, M. Dorrius, X. Xie, et al., The dream of a one-stop-shop: meta-analysis on myocardial perfusion CT, Eur. J. Radiol. (2015).

[8] A. Rossi, D. Merkus, E. Klotz, N. Mollet, P.J. de Feyter, G.P. Krestin, Stress myocardial perfusion: imaging with multidetector CT, Radiology 270 (1) (2014) 25–46.

[9] J.L. Wichmann, F.G. Meinel, U.J. Schoepf, et al., Semiautomated global quantification of left ventricular myocardial perfusion at stress dynamic CT: diagnostic accuracy for detection of territorial myocardial perfusion deficits compared to visual assessment, Acad. Radiol. 23 (4) (2016) 429–437.

[10] P.M. Boiselle, Y.H. Choe, J. Leipsic, F. Pugliese, U.J. Schoepf, R. Vliegenthart, Expert opinion: how and when to perform CT myocardial perfusion imaging, J. Thorac. Imaging 30 (3) (2015) 167–168.

[11] D. Fleischmann, CT angiography: injection and acquisition technique, Radiol. Clin. North Am. 48 (2) (2010) 237 (47, vii).

[12] K.T. Bae, Intravenous contrast medium administration and scan timing at CT: considerations and approaches, Radiology 256 (1) (2010) 32–61.

[13] B. Bischoff, F. Bamberg, R. Marcus, et al., Optimal timing for first-pass stress CT myocardial perfusion imaging, Int. J. Cardiovasc. Imaging 29 (2) (2013) 435–442.

[14] M.D. Cerqueira, N.J. Weissman, V. Dilsizian, et al., Standardized myocardial segmentation and nomenclature for tomographic imaging of the heart. A statement for healthcare professionals from the Cardiac Imaging Committee of the Council on Clinical Cardiology of the American Heart Association, Circulation 105 (4) (2002) 539–542.

[15] R.T. George, M. Jerosch-Herold, C. Silva, et al., Quantification of myocardial perfusion using dynamic 64-detector computed tomography, Invest. Radiol. 42 (12) (2007) 815–822.

[16] B. Ruzsics, H. Lee, E.R. Powers, T.G. Flohr, P. Costello, U.J. Schoepf, Images in cardiovascular medicine: myocardial ischemia diagnosed by dual-energy computed tomography: correlation with single-photon emission computed tomography, Circulation 117 (9) (2008) 1244–1245.

[17] R. Vliegenthart, G.J. Pelgrim, U. Ebersberger, G.W. Rowe, M. Oudkerk, U.J. Schoepf, Dual-energy CT of the heart, AJR Am. J. Roentgenol. 199 (5 Suppl) (2012) S54–S63.